

Reinforcement Learning-Based Dynamic Management of Structured Parallel Farm Skeletons on Serverless Platforms

Lanpei Li ^{*,†} , Massimo Coppola ^{*} , Malio Li [†] , Valerio Besozzi [†] , Jack Bell [†] , Vincenzo Lomonaco [‡] 

^{*}Institute of Information Science and Technologies (ISTI), National Research Council of Italy (CNR), Pisa, Italy

lanpei.li@isti.cnr.it, massimo.coppola@isti.cnr.it

[†]Department of Computer Science, University of Pisa, Pisa, Italy

malio.li@phd.unipi.it, valerio.besozzi@phd.unipi.it, jack.bell@di.unipi.it

[‡]Department of AI, Data and Decision Sciences, LUISS University, Rome, Italy

vlomonaco@luiss.it

Abstract—We present a framework for dynamic management of structured parallel processing skeletons on serverless platforms. Our goal is to bring HPC-like performance and resilience to serverless and continuum environments while preserving the programmability benefits of skeletons. As a first step, we focus on the well known *Farm* pattern and its implementation on the open-source OpenFaaS platform, treating autoscaling of the worker pool as a QoS-aware resource management problem.

The framework couples a reusable farm template with a Gymnasium-based monitoring and control layer that exposes queue, timing, and QoS metrics to both reactive and learning-based controllers. We investigate the effectiveness of AI-driven dynamic scaling for managing the farm’s degree of parallelism via the scalability of serverless functions on OpenFaaS. In particular, we discuss the autoscaling model and its training, and evaluate two reinforcement learning (RL) policies against a baseline of reactive management derived from a simple farm performance model. Our results show that AI-based management can better accommodate platform-specific limitations than purely model-based performance steering, improving QoS while maintaining efficient resource usage and stable scaling behaviour.

I. INTRODUCTION

Serverless Function-as-a-Service (FaaS) platforms promise elastic scaling and operational simplicity, but their black-box autoscalers and cold-start behaviour make it hard to provide performance guarantees for latency-sensitive parallel workloads [1], [2]. In contrast, structured parallel programming frameworks expose high-level skeletons—such as the farm pattern—that decouple application logic from low-level parallel execution and offer a small set of control knobs, most notably the degree of parallelism [3]. Bridging these two worlds requires runtime mechanisms that expose skeleton-level control while coping with platform-specific limitations and overheads.

In this work we study the dynamic management of a task farm skeleton deployed on the open-source OpenFaaS¹ platform.

Corresponding author: Lanpei Li — This research was partially supported by the FIS2 Grant from Italian Ministry of University and Research (Grant ID: FIS2023-03382).

¹See <https://www.openfaas.com>

The farm processes a continuous stream of image-processing tasks under explicit deadline-based quality-of-service (QoS) objectives. We design an OpenFaaS-based farm template, calibrate a workload and QoS model from sequential executions of the image-processing pipeline, and investigate autoscaling policies that adjust the farm’s worker pool size over time in response to non-stationary load, building on and extending prior work on serverless task farming [4], [5].

We contrast analytical reactive baselines derived from a behavioural model of the farm with RL agents that learn scaling policies directly from interaction with the system via a Gymnasium-style environment [6]. Our goal is to understand when AI-based control can compensate for platform-induced delays and non-ideal behaviours that are hard to capture analytically, and how it compares against simple reactive strategies in terms of QoS, efficiency, and stability. Our current evaluation focuses on a single tenant scenario and a single skeleton instance; more complex settings are left to future work. The skeleton, simulation and policy code is open source².

This paper makes the following contributions: (1) Design and implementation of a Farm parallel skeleton (as a specific instance of a Parallel Processing Skeleton) running on the OpenFaaS serverless platform, with Emitter, Worker, and Collector functions connected via Redis-backed queues. (2) Formalisation of a QoS-aware autoscaling problem for the farm skeleton, including a workload and deadline model and a set of metrics capturing performance, efficiency, and QoS. (3) An AI-based dynamic management approach that complements analytical reactive baselines with RL policies aimed at optimising a combination of QoS, resource usage, and scaling stability. (4) Design of the farm autoscaling environment with a set of Gymnasium-style [6] run-time monitoring hooks that expose farm-level state, actions, and rewards for both analytical and learning-based controllers. (5) An experimental comparison on a workload calibrated for an image-processing pipeline. We

²Source code repository: <https://github.com/lilanpei/RL-OpenFaaS-Farm>

evaluate reactive and RL-based policies on top of OpenFaaS in terms of QoS compliance, queue dynamics, and worker utilisation.

The remainder of the paper is organised as follows. Section II positions our work in the context of prior research, briefly reviewing serverless task farms, AI-based autoscaling for Cloud and FaaS platforms, and the reinforcement-learning methods that underpin our methodology. Section III summarizes the options and constraints the OpenFaaS platform provides to our design. Section IV formalises the QoS-aware autoscaling problem for the farm skeleton. Section V presents reactive and RL-based management policies. Section VII details the experimental setup and evaluation, and Section VIII concludes with a summary and future work directions.

II. BACKGROUND

The concept of algorithmic skeletons was first introduced and popularized by Murray [7]. The term *skeleton* refers to the underlying structure or pattern of a parallel algorithm that can be reused across different domains [8]. Algorithmic skeletons are essentially generic, adaptable, and reusable building blocks that can be used to parallelize an application.

Algorithmic skeletons can be broken down into two parts: the semantics of the skeleton and its implementation [9], [10], usually called a *template*.

This separation of concerns explicitly hides implementation details to the application developer, enabling high-level abstraction and portability across different systems and architectures. The actual implementation as a template is the responsibility of the skeleton framework developer [11], [12], who ensures the correctness of the parallelism mechanisms behind the skeletons' templates as well as of their composition properties (“parallelism exploitation correctness ‘by construction’” [13]).

Recent work has started to investigate skeleton-style task farming on serverless platforms. Kehrer et al. [4] introduce serverless skeletons for elastic parallel processing, mapping structured patterns such as task farms onto FaaS backends. Building on this line, Kehrer et al. [5] propose a self-tuning serverless task farming framework with a proactive elasticity controller that adapts parallelism to meet user-defined execution time limits while minimizing cost. Their architectures target parallel task farms and demonstrate that serverless platforms can support elastic parallel patterns when complemented with domain-specific control logic. Complementary benchmarking work by Manner and Wirtz [1] compares resource scaling strategies for open-source FaaS platforms against commercial cloud offerings, highlighting how platform-level scaling choices affect performance and cost.

Our work differs from [1], [4], [5] in several aspects. First, we focus on a structured farm skeleton with explicit QoS guarantees for latency-sensitive stream processing, rather than batch task farms or generic cloud functions. Second, we operate on top of OpenFaaS and expose a Gymnasium-compatible environment for experimentation with different control policies. Third, instead of relying solely on model-based or heuristic controllers, we explore RL agents that

learn autoscaling policies directly from interaction with the environment, while still allowing comparison against reactive, performance-model-based baselines.

AI techniques, and RL in particular, have emerged as promising approaches for cloud autoscaling and resource management. RL agents learn policies that map observed system states to scaling actions in order to optimize long-term reward, which can encode QoS, cost, and stability objectives [14]. Compared to purely rule-based or control-theoretic approaches, RL can adapt to complex, partially unknown dynamics and non-stationary workloads.

RL has been applied to server provisioning and autoscaling in various settings, including data centres and cloud platforms [2], [15], [16]. Concrete RL-based autoscalers have been proposed for Infrastructure-as-a-Service (IaaS) clouds and containerized applications [17]–[19]. These works demonstrate that RL-based controllers can outperform static or threshold-based policies by anticipating load changes and optimizing multi-objective trade-offs. Agarwal et al. [2], for instance, propose a deep reinforcement learning method for autoscaling FaaS functions that jointly considers QoS and cost in a serverless setting. A recent survey [20] and production learning-based autoscaling systems deployed in practice [21], [22] further underscore the maturity and practical relevance of learning-based autoscaling techniques. However, many existing approaches target virtual machines, generic microservices, or individual functions and do not consider the specific semantics of parallel skeletons deployed on serverless FaaS platforms. In this work, we position our RL-based autoscaler in this line of research, but tailor the state representation, action space, and reward shaping to the structured farm skeleton and its QoS constraints.

We adopt two standard value-based RL methods for the farm autoscaling problem, SARSA with eligibility traces and a Double Deep Q-Network (Double DQN) [14], [23], [24], and apply them on a common Gymnasium-style environment interface; their concrete instantiation is detailed in Section V.

When training and comparing different AI techniques over a common experiment, it is essential to decouple environment dynamics from learning algorithms to ease code maintenance and support reproducible studies, so we follow the Gymnasium interface standard [6] for the environment API, which exposes observation and action spaces and allows different RL agents and analytical baselines to be plugged in with minimal changes to the underlying farm deployment.

III. PARALLEL SKELETONS AND THE OPENFAAS SERVERLESS PLATFORM

FaaS platforms like OpenFaaS provide a natural runtime for deploying parallel skeleton stages as independent, serverless functions. OpenFaaS functions are packaged as lightweight Docker containers (function pods) that can be deployed on any Kubernetes-based infrastructure. The platform handles function invocation, scaling, and isolation, freeing developers from managing server processes. This suits our goal of making skeleton instantiation easy and modular: each stage of a pipeline

or each role in a farm can be implemented as a separate function pod, with the skeleton’s logic connecting them. While this work focuses on Farm computation steering, we aim at a larger set of skeletons and have designed the function pods to be generic, reusable, and easily configurable to form other patterns.

Our farm skeleton employs a template (see Sections IV and V) based on three types of functions: the Emitter, the Worker, and the Collector. Each one is a standalone OpenFaaS function (written in Python for our prototype) that knows how to interface with the others. As we detail in Section V, an initial setback was that the invocation mechanisms of the open-source version of OpenFaaS do not provide true scalability or efficient load balancing. Moreover, FaaS advocates for the separation of computation from storage. Consequently, storage access and inter-function communication are achieved via *mediated* channels, often through cloud storage or other indirect mechanisms [25]. Yet, efficient composition of serverless functions in general is complex and, without adding custom runtime support, it breaks the *Serverless Trilemma* [26]. Since OpenFaaS functions are stateless and isolated, we decided to exploit its call semantics only to *activate* pods that would then deal with passing data (tasks and results) between skeleton stages via a separate mechanism.

For this purpose we adopt the same Redis³ distributed queue service also exploited by OpenFaaS as the backbone connecting the function pods, leveraging its performance and proven compatibility. Once activated, each function reads from an input queue and pushes to an output queue, as specified by its skeleton-mandated configuration. This approach decouples producers and consumers, naturally supporting parallelism. Multiple worker instances can compete for tasks on the same queue (thus implementing the farm pattern), and a pipeline can be formed by linking one stage’s output queue to the next stage’s input queue. The use of a fast in-memory queue also enables asynchronous, streaming communication between functions, which is critical for farm and pipeline throughput.

By changing configuration (e.g. queue names, or environment flags), the same function pods can already be deployed and composed in different ways, enabling any combination of farms and pipelines while keeping the core logic the same. Additional pod designs can be easily coded to support other skeletons and templates.

IV. PROBLEM FORMULATION

We consider a single instance of the stream-based *farm skeleton* computational pattern [3], to be deployed on the OpenFaaS serverless platform. We adopt the same classic template as the cited FastFlow implementation comprising an input stage, a pool of parallel workers, and an output stage. In this work we focus on the worker pool size as the sole control parameter for dynamic resource management, while keeping all other configuration options fixed. In our template the worker pool size is constrained to an interval $N_{\min} \leq N_k \leq N_{\max}$ and can only be adjusted at discrete control steps separated

by a fixed step duration T_{step} . At each step k , the controller issues a scaling action that changes the worker count by a small integer increment (scale down, no-op, scale up). In practice, the OpenFaaS deployment introduces non-negligible scale-up delay due to function and queue-worker initialization (see Section V), so the effect of large scaling actions on the effective worker pool may be smoothed over multiple steps.

Generic performance models of the farm skeleton are well studied and provide the foundation for dynamically steering resource allocation by selecting the next action according to the skeleton status. We gather a set of metrics that allow both reactive and RL-based policies to be evaluated and trained, capturing the internal state, resource allocation, and performance behaviour.

At each control step k we summarize the farm state as

$$\mathbf{s}_k = [|Q_{in,k}|, |Q_{work,k}|, |Q_{res,k}|, |Q_{out,k}|, N_k, \bar{T}_{proc,k}, T_{proc,k}^{max}, \lambda_{a,k}, q_k]^\top \in \mathbb{R}^9. \quad (1)$$

Here all symbols with subscript k denote quantities measured at control step k : $|Q_{...,k}|$ are queue lengths, $\bar{T}_{proc,k}$ is the moving average of recent processing times, $T_{proc,k}^{max}$ is the maximum observed processing time in a sliding window, $\lambda_{a,k}$ is the moving average arrival rate, and q_k is the instantaneous QoS defined as the fraction of tasks meeting their service time deadline within the step. From these, we can derive three broad performance objectives:

- **QoS**: ensure a set fraction of tasks complete before their deadlines, keeping the QoS above a target level q^* .
- **Responsiveness**: limit work backlog and latency by reacting to queue build-up and related waiting times.
- **Efficiency**: minimize the average of active Workers and avoid excessive scaling actions while meeting QoS.

The dynamic scaling problem can thus be cast as a sequential decision problem: at each control step, the autoscaler observes the current farm state and chooses a scaling action according to a given policy that balances the tradeoff between QoS, responsiveness, and efficiency over time.

The farm workload in our experiments is a stream of image processing tasks that are described in Section VII. Each task τ_i arrives at time t_i^{arr} with an associated input size s_i (length in pixels of the side of a square image) and an expected sequential processing time $\hat{T}_s(s_i)$. We set a deadline D_i for each task as a multiple of the expected duration,

$$D_i = \beta \cdot \hat{T}_s(s_i) \quad (2)$$

where $\beta > 1$ is a slack coefficient (we set $\beta = 2$ in all experiments). A task is said to meet its QoS requirement if its completion time C_i satisfies $C_i - t_i^{arr} \leq D_i$. Over a control interval, we track the fraction of tasks that meet their deadlines as the instantaneous QoS level q_k at control step k .

We model the scaling problem as a Markov Decision Process (MDP) described as a tuple $\langle \mathcal{S}, \mathcal{A}, \mathcal{P}, \mathcal{R}, \gamma \rangle$ [14], where the elements are respectively state space, action space, transition function, reward function, and discount factor. The concrete

³See <https://redis.io/docs/latest/>

realization of this MDP as a Gymnasium environment is described in Section V-D. The objective is to find the optimal policy π^* that maximizes the cumulative reward:

$$\pi^* = \arg \max_{\pi} \mathbb{E} \left[\sum_{k=1} \mathcal{R}_k^\pi \right] \quad (3)$$

where \mathcal{R}_k^π is the reward obtained following policy π at control step k . To match the performance objectives with Eq. 3, we designed the reward function accordingly (Eq. 4 in Fig. 3).

V. FARM SKELETON IMPLEMENTATION

The farm skeleton is implemented on OpenFaaS following the FastFlow [3] Farm template, comprising Emitter, Workers, and Collector components that handle image-analysis workloads under dynamic load conditions. The template separates generation, parallel processing, and aggregation; we retain this structure and connect stages via Redis-backed queues. An initial “one-function-name with multiple replicas” mapping in OpenFaaS led to unbalanced pod utilization, motivating the customized invocation and scaling workflow described in the next subsection.

The farm implementation consists of three OpenFaaS functions and an external autoscaling environment (orchestrator), as illustrated in Fig. 1.

The queues (`input_queue` → `worker_queue` → `result_queue` → `output_queue`) realize the bounded buffers between stages, providing natural back-pressure and decoupling producer/consumer rates. All functions use a shared `program_start_time` for consistent relative timestamps. In addition to these data queues, a dedicated set of control queues (e.g., `start-queue`) connects the environment with the Emitter, Workers, and the Collector for lifecycle and scaling commands (e.g., `start`, `scale`, `terminate`).

A. Customized Invocation and Scaling

A straightforward strategy that invoked a single function name with multiple replicas and relied on OpenFaaS/Kubernetes Services for load balancing led to uneven utilization, with the gateway reusing HTTP keep-alive connections to a single pod and leaving others idle under load.

To obtain deterministic load distribution and explicit control over scaling, we instead deploy N distinct worker functions (worker-1, ..., worker- n), each with a single replica, and invoke them asynchronously via the OpenFaaS API under the control of the external environment. Each invocation maps one-to-one onto a pod and launches a long-running handler loop, potentially keeping the worker function alive indefinitely. The environment manages scale-up and scale-down as one-step changes in the active worker set while preserving in-flight work.

The asynchronous call strategy that allows managed scaling in our design requires a one-to-one pairing between each Worker function and a dedicated queue-worker replica that drives its asynchronous invocation throughout the Worker's lifecycle. The dedicated queue manager is necessary to decouple function execution from HTTP connection lifetimes, and prevent opportunistic termination or scale-to-zero of long-running handlers by OpenFaaS.

In practice, end-to-end scale-up for a single Worker takes about 5 to 8 seconds (covering Kubernetes scheduling, function cold start, queue-worker startup, and completing the handshake), but the overall time grows approximately linearly with the number of Workers. The trade-off of efficient task distribution is a near-linear scale-up latency that can challenge timely reactions to high load. Under abrupt load spikes, the orchestrator may therefore lag in raising capacity quickly enough, leading to transient queue growth and an elevated risk of missed deadlines.

B. Function and Process Realization

Emitter. The Emitter receives tasks from outside the skeleton and dispatches them to the Workers. In our simulation we also integrate task production into this component to avoid unnecessary Redis overhead. The Emitter pod reads per-phase descriptors from the `input_queue`, generates tasks with controlled stochastic timing, and enqueues them into the `worker_queue`. It runs as a long-lived loop and supports seeded runs for reproducibility.

Workers (W_1, W_2, \dots, W_N) form a pool of functions that compute in parallel. Each Worker pulls tasks from the `worker_queue`, executes the image-processing pipeline, records processing times, and sends results to `result_queue`. Control signals from the environment govern when Workers are added, drained, or terminated, but the data path remains a simple pull–process–push loop.

Collector. The Collector consumes completed tasks from the `result_queue` and dispatches them to the `output_queue`. Additional farm semantics (e.g. task reordering) are not needed in our experiments, but the Collector hosts monitoring code. In our prototype it reconstructs end-to-end timings relative to `program_start_time`, evaluates QoS against per-task deadlines, annotates the output, and logs QoS status. It also participates in synchronizations to align the time origin at skeleton startup and shutdown.

Orchestrator. The Orchestrator implements the autoscaling environment of Section V-D and hosts the autoscaler. It runs outside the OpenFaaS functions, periodically reading queue

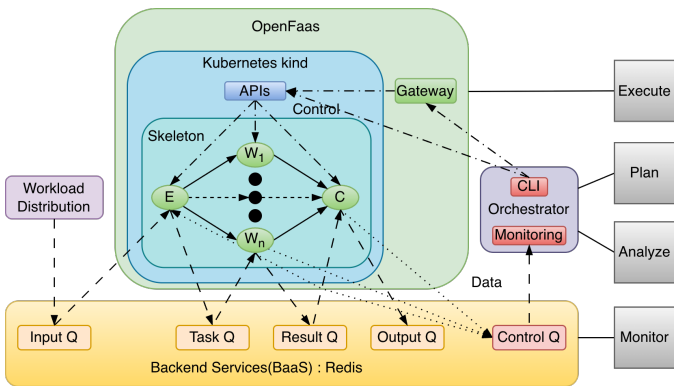


Fig. 1. OpenFaaS-based farm skeleton template.

lengths, worker counts, timing summaries, and QoS indicators, and forwards them to an autoscaler implemented either as a reactive baseline (ReactiveAverage, ReactiveMaximum or as a reinforcement-learning agent (SARSA, DQN in Section VI-A). The selected policy then issues scale-up/scale-down requests through the OpenFaaS API. This Gymnasium-style control layer keeps the farm data path separate from the management plane, as detailed in Section V-D.

C. Workload and QoS Modeling

The workload follows a four-phase arrival pattern introduced in Section VII, combining phases with different steady and oscillatory regimes as summarized in Fig. 4 and Tab. II. Each task is annotated with an expected processing time and a derived deadline from the calibrated image-processing model, and QoS decisions in the Collector compare completion times against these deadlines. Optional phase shuffling supports robustness experiments.

D. Autoscaling Environment

The environment provides a Gymnasium-style interface for experimentation with reinforcement learning and reactive baselines. The observation vector S defined by Eq. 1 comprises queue depths, worker count, timing summaries, estimated arrival rates, and QoS indicators. Actions are single-step deltas in the worker pool size, clipped to configured bounds ($\mathcal{A} = \{-1, 0, +1\}$) and subject to step-duration constraints. The environment deploys and invokes functions, manages queue-worker capacity, and returns per-step information such as queue depths, current workers, processing-time summaries, estimated arrival rate, and QoS success rate as a 9-element vector. The reward function combines QoS tracking, backlog control, worker efficiency, and scaling friction with configurable weights and thresholds. This external control layer keeps scaling orthogonal to the farm’s data plane, enabling reproducible studies under identical pipeline semantics.

E. Implementation Considerations and Limitations of the Farm Skeleton on OpenFaaS

We ensure resilient Redis operations for queue interactions, employing safe calls and limited retries to handle transient errors without violating pipeline invariants. Control channels are separated from data queues to simplify reasoning about liveness and safety. On scale-up, the environment coordinates worker-service deployment with adjustments to the OpenFaaS queue-worker so that asynchronous invocations are not delayed. All components timestamp events are relative to `program_start_time`, ensuring coherent end-to-end tracking across functions and enabling precise QoS evaluation.

To validate the correctness and scalability of the farm skeleton implementation, we first run experiments with varying numbers of workers and workload configurations. Fig. 2 summarizes runtime and initialization overheads, showing that while task runtime decreases with increasing parallelism, farm initialization time grows with the number of Workers. While in infinite-stream settings initialization can be ignored, the

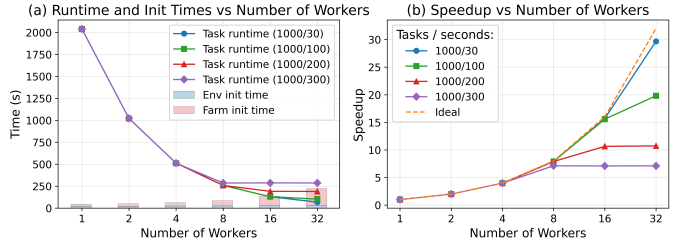


Fig. 2. Scaling metrics for the farm skeleton: runtime, initialization overhead (left) and speedup (right) vs. worker count, under static workloads.

OpenFaaS-induced scale-up latency imposes a practical ceiling on effective parallelism for finite streams as well as dynamically varying workloads, motivating the need for autoscaling policies that trade off throughput gains against initialization costs.

VI. FARM DYNAMIC MANAGEMENT POLICIES

We now define the autoscaling policies used in our experiments: analytical reactive baselines and learning-based agents. We implemented two analytical baselines that compute the required parallelism directly from queue lengths and service-time estimates. Both policies consume the environment observation vector and output an action in $\{-1, 0, +1\}$ via the environment’s discrete mapping.

ReactiveAverage (RA) uses the average processing time as the service-time estimate. It plans over a finite horizon and provisions capacity for both clearing the current backlog and serving expected arrivals. Let `service_time` be the average processing time and `horizon` the planning window. It computes workers for arrivals as $arrival_rate * service_time$ and workers for backlog as $(worker_q/horizon) * service_time$. A mirrored enqueue counter provided by the environment is used to estimate active tasks and convert them into effective busy capacity, which refines the idleable capacity before mapping the difference to a discrete action.

ReactiveMaximum (RM) mirrors the above logic but uses the maximum observed processing time in the state. It emphasizes QoS protection by provisioning against worst-case service time. Both policies maintain negligible computational overhead and require no training, making them useful baselines and operationally attractive when training is not possible.

To clarify the impact of reward shaping, we note that the main weights in Eq. (4) act as intuitive knobs that shift the QoS-cost-stability trade-off. Increasing w_{qos} and $w_{backlog}$ makes the controller more aggressive in matching deadlines and suppressing queue growth, typically at the cost of higher mean workers and more frequent scale-ups. Increasing w_{scale} discourages reconfigurations and can improve stability, but if set too high it delays corrective actions and may reduce QoS under fast load changes. The efficiency term w_{eff} mainly affects low-load behaviour by encouraging scale-down once QoS is satisfied and Q_k is small, while the directional incentives (w_{up} , w_{down}) bias the policy toward earlier scale-up or more conservative scale-down. In our evaluation we keep the reward coefficients fixed to enable controlled comparisons across policies.

$$\begin{aligned}
R_k = & \underbrace{w_{\text{qos}}(q_k - q^*)}_{\text{QoS tracking}} - \underbrace{w_{\text{backlog}} \left(\frac{Q_k}{Q^*} - 1 \right)^2}_{\text{Queue/backlog penalty}} - \underbrace{w_{\text{scale}}}_{\text{Scaling cost}} \\
& - \underbrace{w_{\text{eff}} \mathbf{1}[Q_k \leq Q_{\text{idle}}, q_k \geq q^*] \max(0, N_k - N^*)}_{\text{Over-provisioning penalty}} \\
& + \underbrace{w_{\text{up}} \mathbf{1} \left[\Delta N_k > 0, \left(\frac{Q_k}{Q^*} > 1 \text{ or } q_k < q^* \right) \right]}_{\text{Reward for justified scale-up}} \\
& + \underbrace{w_{\text{down}} \mathbf{1} \left[\Delta N_k < 0, \left(\frac{Q_k}{Q^*} \leq 1 \text{ and } q_k \geq q^* \right) \right]}_{\text{Reward for safe scale-down}} \\
& + \underbrace{w_{\text{qos}} \mathbf{1} \left[q_k \geq q^*, \frac{Q_k}{Q^*} \leq 0.5 \right]}_{\text{Bonus for stable high-QoS operation}}. \quad (4)
\end{aligned}$$

Fig. 3. The reward function for SARSA and DQN

A. AI Approach: SARSA and DQN

We instantiate two standard value-based RL agents for scaling: a tabular SARSA(λ) controller over a discretized state space and a lightweight Double DQN operating on the continuous observation vector, following established formulations for SARSA and deep Q-learning. Both interact with the same Gymnasium-style environment V-D, consume the state vector s_k defined in Eq. 1, and act on the same discrete scaling actions $\mathcal{A} = \{-1, 0, +1\}$. SARSA uses a discretized state representation with eligibility traces, whereas Double DQN uses a small MLP over continuous observations; in both cases we keep hyperparameters fixed across all evaluation runs.

To connect these autoscaling objectives to a learnable signal, we define a shaped reward that combines four primary components: QoS tracking relative to a target rate, queue backlog relative to a healthy target, worker efficiency relative to a balanced target, and a penalty on scaling events.

Equation (4) in Fig. 3 defines a shaped reward that balances service quality, backlog control, resource efficiency, and stability. The terms jointly reward high QoS and justified scale-up/scale-down decisions while penalizing backlog overflow, over-provisioning, and unnecessary scaling, guiding the agent toward timely but non-oscillatory scaling behavior.

VII. EXPERIMENTAL SETTINGS

Our use case is an image-processing application with variable image sizes, implemented as a four-stage sequential pipeline (thumbnail generation, compression, metadata extraction, and format conversion). This provides a concrete workload whose service time scales with image size and underpins our QoS-deadline model.

To obtain hardware-agnostic service times, we profile the full pipeline on a reference host for the relevant image sizes and fit a reduced quadratic model from image size to end-to-end

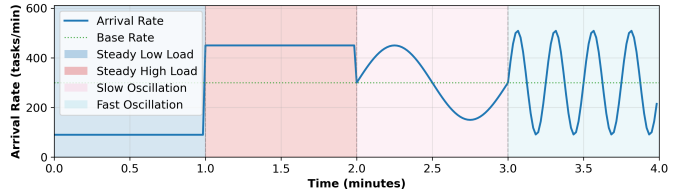


Fig. 4. Configured mean of task arrival patterns across four workload phases.

time. Table I reports the resulting expected times and default QoS deadlines used in the experiments.

In the farm simulation, each Worker emulates processing via `time.sleep(processing_time)`, which allows us to isolate the impact of the autoscaling policy and OpenFaaS control-plane latencies. This abstracts away compute contention (e.g., CPU saturation and cache/memory effects) and noisy network/storage conditions, so the results primarily characterise the controller’s ability to cope with OpenFaaS control-plane latencies and queueing dynamics rather than compute-bound interference.

A. Task Arrival Patterns and Sizes

The workload process is designed to stress control rather than compute. We use a weighted random distribution of per-task work size, so that the mean task computational load is fixed to 1.5s (a stochastic stationary behaviour). We modulate the arrival rate across four phases (steady low, steady high, slow oscillation, fast oscillation) as summarized in Fig. 4 and Table II. Within each phase we thus generate stochastic arrivals as a Poisson process (exponentially distributed inter-arrival times) with phase-appropriate rate, and enforce an exact per-phase task count via short windows with the final window adjusted to match the target total.

TABLE I
EXAMPLE OF EXPECTED MODEL OUTPUTS T_s AND QOS DEADLINES

Image Size	512x512	1Kx1K	2Kx2K	4Kx4K
Expected time	0.046 s	0.181 s	0.719 s	2.870 s
Default deadline ($\beta = 2$)	0.09 s	0.35 s	1.42 s	5.58 s

TABLE II
TASK ARRIVAL PATTERNS IN THE FOUR PHASES OF EACH EPISODE.

Phase, Arrival pattern	Load wrt base level	Avg. Tasks /min.	Cycles /Phase	Typical intent
0: Steady Low Load, Poisson	0.3	90	-	Idle regime, for stability checks
1: Steady High Load, Poisson	1.5	450	-	Sustained heavy load, test scale-up capacity
2: Slow Oscillation, Sinusoidal Poisson	0.5–1.5	300	1	Smooth fluctuations, test tracking
3: Fast Oscillation, Sinusoidal Poisson	0.3–1.7	300	4	Rapid bursts, test responsiveness, damping

B. Evaluation Methodology

Each policy was evaluated over 10 independent episodes (240 seconds each) with different random seeds. Table III summarises metrics over the episodes (mean \pm standard deviation) for the four scaling policies, reporting QoS success rate (fraction of tasks meeting deadlines), resource usage, and stability (scaling actions and no-ops).

The learning-based agents clearly outperform the reactive baselines in final QoS: SARSA reaches $99.20\% \pm 0.52\%$ and DQN $94.91\% \pm 3.79\%$, whereas RA and RM achieve only $50.87\% \pm 4.38\%$ and $65.61\% \pm 14.26\%$, respectively. SARSA therefore offers the strongest guarantees, and DQN still improves QoS by more than 40 percentage points over both reactive policies. This strong SARSA performance, however, relies on a carefully designed discretisation of the observation space, whereas DQN operates directly on the continuous observation vector, trading a small QoS loss for a simpler interface between environment and controller.

Table III also helps pinpoint where each policy succeeds or fails under the four arrival regimes. SARSA maintains near-perfect QoS in every phase while keeping mean workers in the mid-teens, indicating that it scales up promptly in the sustained high-load phase and scales down again during oscillatory phases without accumulating backlog. DQN attains similarly high QoS in three phases but drops during sustained high load, consistent with its conservative scaling behaviour (few reconfigurations) and the non-negligible OpenFaaS scale-up latency, which together can delay capacity increases when the load remains high. The reactive baselines show their largest degradation in the steady high-load phase: despite scaling activity, they under-provision relative to the sustained arrival rate, leading to large queues and missed deadlines; their partial recovery in oscillatory phases reflects that the load periodically returns to more manageable levels.

The QoS–resource trade-off in Fig. 5 (up) shows that SARSA combines the highest QoS with moderate average workers, whereas DQN uses similar capacity but settles at a slightly lower QoS. The reactive baselines either under-provision (RA) or spend comparable capacity without matching the QoS of

TABLE III
COMPARISON OF FARM SCALING POLICIES WITH REACTIVE BASELINES
OVERALL AND AS PER-PHASE AGGREGATES OF QOS AND MEAN WORKERS.
ALL METRICS REPORTED AS MEAN \pm STD OVER 10 RUNS.

Phase	Metric	SARSA	DQN	ReactiveAvg	ReactiveMax
	Final QoS [%]	99.20 ± 0.52	94.91 ± 3.79	50.87 ± 4.38	65.61 ± 14.26
	Mean Workers	14.78 ± 0.49	14.40 ± 0.77	10.79 ± 0.31	13.92 ± 0.68
	Max Workers	17.80 ± 0.75	15.60 ± 1.02	16.60 ± 0.66	18.80 ± 0.40
	Scaling Actions	24.00 ± 2.05	3.60 ± 1.02	28.40 ± 0.92	26.80 ± 1.25
	No-op Actions	4.90 ± 1.92	24.60 ± 1.69	1.00 ± 1.00	1.70 ± 0.78
0	QoS [%]	99.7 ± 0.5	99.2 ± 1.1	91.3 ± 4.7	91.0 ± 5.1
	mean workers	14.26 ± 0.31	12.01 ± 0.04	8.11 ± 0.14	8.91 ± 0.59
1	QoS [%]	99.0 ± 0.8	90.1 ± 7.5	2.0 ± 2.9	27.0 ± 32.4
	mean workers	16.66 ± 0.35	14.54 ± 1.12	10.30 ± 0.98	12.88 ± 1.63
2	QoS [%]	99.8 ± 0.2	99.9 ± 0.2	76.6 ± 17.1	95.8 ± 10.6
	mean workers	13.36 ± 0.90	15.60 ± 1.02	14.44 ± 1.30	17.27 ± 0.46
3	QoS [%]	99.7 ± 0.3	99.9 ± 0.3	93.0 ± 4.6	100.0 ± 0.1
	mean workers	14.63 ± 1.20	15.60 ± 1.02	10.39 ± 0.46	16.96 ± 0.89

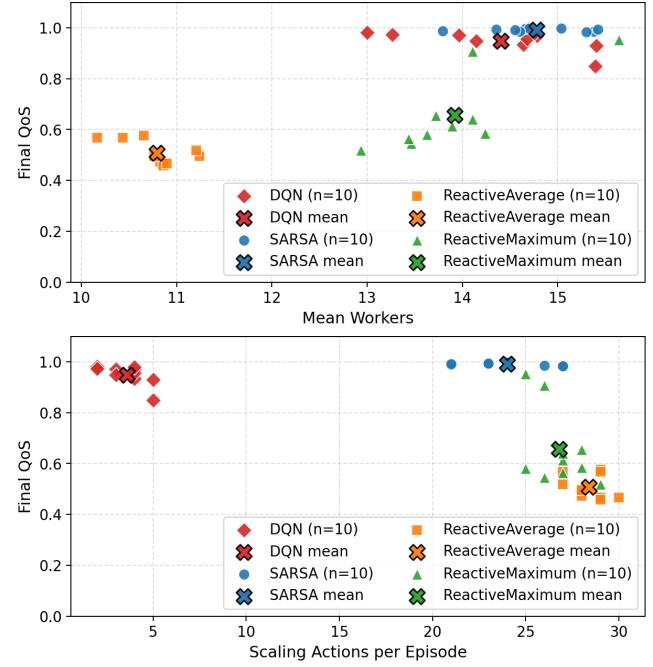


Fig. 5. Final QoS vs. mean workers (up) and number of scaling actions (down), over 10 runs (per-run points and overall average).

the learning-based policies (RM). Fig. 5 (down) highlights that SARSA reaches near-optimal QoS with fewer scaling actions than the reactive baselines, while DQN achieves high QoS with very few reconfigurations. Under common pricing models [27], the learning-based agents provide more favourable QoS–cost trade-offs than the reactive baselines by sustaining higher QoS with moderate capacity and fewer ineffective reconfigurations.

Finally, Fig. 6 shows the temporal evolution of the policies across the four workload phases. Both learning-based agents maintain high QoS where the reactive baselines collapse during high-load or rapidly varying phases despite aggressive scaling, confirming that simple threshold-based rules are insufficient to capture the temporal structure of the workload when the action range is constrained. Overall, these results demonstrate that model-free reinforcement learning yields autoscaling policies that dominate reactive heuristics in the QoS–cost–stability space: SARSA provides the strongest QoS guarantees, while DQN offers a nearby operating point characterised by very low scaling activity and slightly relaxed QoS targets.

VIII. CONCLUSIONS

This work presented an OpenFaaS-based implementation of a structured-parallel Farm skeleton together with an external autoscaling environment, formalised autoscaling as a Markov decision process with QoS-aware deadlines for an image-processing workload, and introduced a shaped reward that trades off service quality, backlog, worker usage, and scaling stability. We evaluated tabular SARSA(λ) and Double DQN controllers against reactive baselines in a single-tenant deployment of a single Farm skeleton, using calibrated sleep-based service-time emulation. Experiments show that learning-based

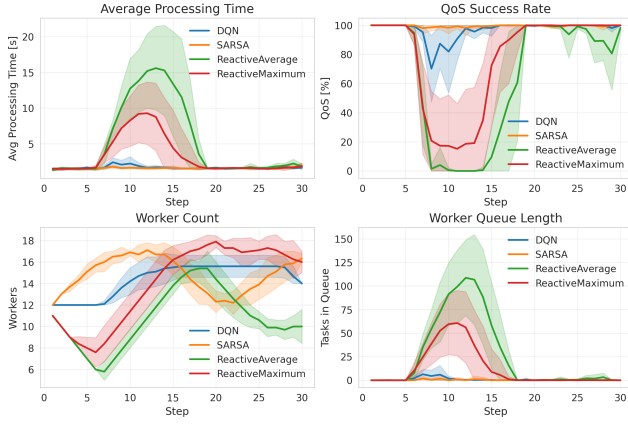


Fig. 6. Policy comparison: SARSA and DQN vs. reactive baselines, showing mean $\pm\sigma$ of \bar{T}_{proc} , running QoS, instantaneous worker count, and worker-queue length Q_{worker} over episode steps.

policies consistently outperform reactive thresholds: SARSA attains near-perfect deadline satisfaction with moderate worker usage and fewer reconfigurations, while DQN trades a small QoS degradation for very few scaling actions and high stability. Future work will address further validation by evaluating multi-tenant settings, compositions of multiple interacting skeletons, actual workloads versus sleep-based emulation, and more challenging arrival processes including different distributions, impulse stress tests and real-world traffic traces.

REFERENCES

- [1] J. Manner and G. Wirtz, "Resource scaling strategies for open-source FaaS platforms compared to commercial cloud offerings," in *2022 IEEE 15th International Conference on Cloud Computing (CLOUD)*, 2022, pp. 40–48. [Online]. Available: <https://doi.org/10.1109/CLOUD55607.2022.00020>
- [2] S. Agarwal, M. A. Rodriguez, and R. Buyya, "A deep recurrent-reinforcement learning method for intelligent autoscaling of serverless functions," *IEEE Transactions on Services Computing*, vol. 17, no. 5, pp. 1899–1910, 2024. [Online]. Available: <https://doi.org/10.1109/TSC.2024.3387661>
- [3] M. Aldinucci, M. Danelutto, P. Kilpatrick, and M. Torquati, "Fastflow: High-level and efficient streaming on multicore," in *Programming Multicore and Many-core Computing Systems*, S. Pllana and F. Xhafa, Eds. Wiley, 2017, pp. 261–280.
- [4] S. Kehrer, J. Scheffold, and W. Blochinger, "Serverless skeletons for elastic parallel processing," in *2019 IEEE 5th International Conference on Big Data Intelligence and Computing (DATACom)*, Kaohsiung, Taiwan, 2019, pp. 185–192. [Online]. Available: <https://doi.org/10.1109/DataCom.2019.00036>
- [5] S. Kehrer, D. Zietlow, J. Scheffold, and W. Blochinger, "Self-tuning serverless task farming using proactive elasticity control," *Cluster Computing*, vol. 24, no. 2, pp. 799–817, 2021.
- [6] M. Towers, A. Kwiatkowski, J. Terry, J. U. Balis, G. De Cola, T. Deleu, M. Goulão, A. Kallinteris, M. Krimmel, A. KG *et al.*, "Gymnasium: A standard interface for reinforcement learning environments," *arXiv preprint arXiv:2407.17032*, 2024.
- [7] M. Cole, *Algorithmic skeletons: structured management of parallel computation*. Pitman London, 1989.
- [8] A. E. Chis and H. González-Vélez, *Design Patterns and Algorithmic Skeletons: A Brief Concordance*. Springer International Publishing, 2018, pp. 45–56. [Online]. Available: https://doi.org/10.1007/978-3-319-73767-6_3
- [9] M. McCool, A. D. Robison, and J. Reinders, "Chapter 1 - introduction," in *Structured Parallel Programming*, M. McCool, A. D. Robison, and J. Reinders, Eds. Boston: Morgan Kaufmann, 2012, pp. 1–38.
- [10] D. B. Skillicorn, "Towards a higher level of abstraction in parallel programming," in *Proc. of the Conf. on Programming Models for Massively Parallel Computers*, ser. PMMP '95. USA: IEEE, 1995, p. 78.
- [11] J. Fang, C. Huang, T. Tang, and Z. Wang, "Parallel programming models for heterogeneous many-cores: a comprehensive survey," *CCF Trans. on High Performance Computing*, vol. 2, no. 4, pp. 382–400, Dec. 2020.
- [12] H. González-Vélez and M. Leyton, "A survey of algorithmic skeleton frameworks: high-level structured parallel programming enablers," *Softw. Pract. Exper.*, vol. 40, no. 12, pp. 1135–1160, nov 2010. [Online]. Available: <https://doi.org/10.1002/spe.1026>
- [13] M. Danelutto, G. Mencagli, M. Torquati, H. González-Vélez, and P. Kilpatrick, "Algorithmic skeletons and parallel design patterns in mainstream parallel programming," *International Journal of Parallel Programming*, vol. 49, no. 2, pp. 177–198, 2021. [Online]. Available: <https://doi.org/10.1007/s10766-020-00684-w>
- [14] R. S. Sutton and A. G. Barto, *Reinforcement Learning: An Introduction*, 2nd ed. Cambridge, MA: MIT Press, 2018.
- [15] G. Tesauro, N. K. Jong, R. Das, and M. N. Bennani, "A hybrid reinforcement learning approach to autonomic resource allocation," in *Proceedings of the IEEE International Conference on Autonomic Computing (ICAC 2006)*. IEEE, 2006, pp. 65–73.
- [16] H. Mao, M. Alizadeh, I. Menache, and S. Kandula, "Resource management with deep reinforcement learning," in *Proceedings of the 15th ACM Workshop on Hot Topics in Networks (HotNets '16)*. New York, NY, USA: ACM, 2016, pp. 50–56.
- [17] E. Barrett, E. Howley, and J. Duggan, "Applying reinforcement learning towards automating resource allocation and application scalability in the cloud," *Concurrency and Computation: Practice and Experience*, vol. 25, no. 12, pp. 1656–1674, 2013.
- [18] A. A. Khaleq and I. Ra, "Intelligent Autoscaling of Microservices in the Cloud for Real-Time Applications," *IEEE Access*, vol. 9, pp. 35 464–35 476, 2021.
- [19] J. Santos, E. Reppas, T. Wauters, B. Volckaert, and F. De Turck, "Gwydion: Efficient auto-scaling for complex containerized applications in Kubernetes through Reinforcement Learning," *Journal of Network and Computer Applications*, vol. 234, p. 104067, Feb. 2025.
- [20] Y. Garí, D. A. Monge, E. Pacini, C. Mateos, and C. G. Garino, "Reinforcement learning-based application autoscaling in the cloud: A survey," *Engineering Applications of Artificial Intelligence*, vol. 102, p. 104288, 2021. [Online]. Available: <https://doi.org/10.1016/j.engappai.2021.104288>
- [21] H. Qiu, W. Mao, C. Wang, H. Franke, A. Youssef, Z. T. Kalbarczyk, T. Başar, and R. K. Iyer, "AWARE: Automate workload autoscaling with reinforcement learning in production cloud systems," in *2023 USENIX Annual Technical Conference (USENIX ATC 23)*, 2023, pp. 387–402.
- [22] K. Rzadca, P. Findeisen, J. Swiderski, P. Zych, P. Broniek, J. Kusmierk, P. Nowak, B. Strack, P. Witkowski, S. Hand, and J. Wilkes, "Autopilot: workload autoscaling at Google," in *Proceedings of the 15th European Conference on Computer Systems*, ser. EuroSys '20. New York, NY, USA: Association for Computing Machinery, Apr. 2020, pp. 1–16.
- [23] V. Mnih, K. Kavukcuoglu, D. Silver, A. A. Rusu *et al.*, "Human-level control through deep reinforcement learning," *Nature*, vol. 518, no. 7540, pp. 529–533, 2015. [Online]. Available: <https://doi.org/10.1038/nature14236>
- [24] H. Van Hasselt, A. Guez, and D. Silver, "Deep reinforcement learning with double q-learning," in *Proceedings of the AAAI conference on artificial intelligence*, vol. 30, 2016.
- [25] M. Copik, R. Böhringer, A. Calotoiu, and T. Hoefler, "FMI: Fast and Cheap Message Passing for Serverless Functions," in *Proceedings of the 37th ACM International Conference on Supercomputing*, ser. ICS '23. ACM, 2023, pp. 373–385. [Online]. Available: <https://doi.org/10.1145/3577193.3593718>
- [26] I. Baldini, P. Cheng, S. J. Fink, N. Mitchell, V. Muthusamy, R. Rabbah, P. Suter, and O. Tardieu, "The serverless trilemma: Function composition for serverless computing," in *Proceedings of the 2017 ACM SIGPLAN International Symposium on New Ideas, New Paradigms, and Reflections on Programming and Software*, 2017, pp. 89–103. [Online]. Available: <https://doi.org/10.1145/3133850.3133855>
- [27] S.-H. Chun, "Cloud services and pricing strategies for sustainable business models: analytical and numerical approaches," *Sustainability*, vol. 12, no. 1, p. 49, 2019. [Online]. Available: <https://doi.org/10.3390/su12010049>